

SLIP: Securing LLM’s IP Using Weights Decomposition

Yehonathan Refael^{*1}, Adam Hakim¹, Lev Greenberg¹, Tal Aviv¹, Satya Lokam¹, Ben Fishman¹, and Shachar Seidman²

¹Microsoft

July 16, 2024

Abstract

Large language models (LLMs) have recently seen widespread adoption, in both academia and industry. As these models grow, they become valuable intellectual property (IP), reflecting enormous investments by their owners. Moreover, the high cost of cloud-based deployment has driven interest towards deployment to edge devices, yet this risks exposing valuable parameters to theft and unauthorized use. Current methods to protect models’ IP on the edge have limitations in terms of practicality, loss in accuracy, or suitability to requirements. In this paper, we introduce a novel hybrid inference algorithm, named SLIP, designed to protect edge-deployed models from theft. SLIP is the first hybrid protocol that is both practical for real-world applications and provably secure, while having zero accuracy degradation and minimal impact on latency. It involves partitioning the model between two computing resources, one secure but expensive, and another cost-effective but vulnerable. This is achieved through matrix decomposition, ensuring that the secure resource retains a maximally sensitive portion of the model’s IP while performing a minimal amount of computations, and vice versa for the vulnerable resource. Importantly, the protocol includes security guarantees that prevent attackers from exploiting the partition to infer the secured information. Finally, we present experimental results that show the robustness and effectiveness of our method, positioning it as a compelling solution for protecting LLMs.

1 Introduction

Large Language Models (LLMs) are increasingly being commercialized due to their superior performance and vast applications [83]. Alongside this trend, many researchers have been tackling challenges related to their deployment – balancing costs, latency, performance and security. Companies developing LLMs invest substantial capital to create these models, mostly in extensive computing resources for training, which could reach hundreds of millions of dollars [54], but also on high-end talent, datasets and labeling, proprietary training procedures and unique network architecture. Consequently, the parameters of a pre-trained foundational model can be considered *highly valuable* intellectual property (IP) for its owner, who would therefore be highly motivated to secure it from theft. Hosting the models on cloud services may offer considerable security against various theft

^{*}Author worked on this research during his internship at Microsoft.

⁰Email addresses: Yehonathan Refael (t-yrefael@microsoft.com), Adam Hakim (adamhakim@microsoft.com), Lev Greenberg (levgreenberg@microsoft.com), Tal Aviv (talaviv@microsoft.com), Shachar Seidman (v-sseidman@microsoft.com), Ben Fishman (ben.fishman@microsoft.com), Satya Lokam (satya.lokam@microsoft.com).

and extraction attacks, but the costs associated with these services can become exorbitant with the exponential growth in demand [50]. As a result, there is a growing financial incentive to offload some, or even most, of the computational work from secure computing resources, like the cloud, to more cost-effective, but *less secure* edge devices, such as servers, laptops, and smartphones. However, model owners seeking to utilize this affordable and accessible computing resource need a security solution that ensures their valuable intellectual property remains safe.

Recently, hybrid inference has been emerging as a framework that aims to address various challenges related to deployment of LLM’s [12]. In this framework, tokens are generated by two computing resources that differ in certain properties, with most strategies focusing on cost and performance [17, 1, 35], or on privacy [28, 10, 59], rather than on model security. Few have aimed to protect model IP; For example, in [63] they propose securing final layers of DNNs, but their approach offers only a single cutoff point in the model, supports feed-forward DNNs only, degrades performance and requires retraining which cannot guarantee information leakage. [85] uses RL for model splitting but, but their obfuscated parameters are inefficiently spread across the model, and they lack security guarantees against recovery through observing inferences. [41] employs weight permutation and an authorization module on a trusted execution environment (TEE), but is not provably secure, vulnerable to hardware attacks and impractical for consumer devices due to the cost of TEEs.

In this paper, we propose a novel approach based on *hybrid inference*, which we name SLIP 1, that addresses this problem and enables utilization of a cheap and low-security computing resource in tandem with an expensive resource that has higher security guarantees. our hybrid inference approach provides a versatile and economical solution for leveraging the full capabilities of LLMs while accommodating various budget constraints, latency and security standards, with no loss in model accuracy. We achieve this by offloading the majority of computations to the cost-effective but less secure computing resource, while protecting the most valuable yet computationally undemanding information on the secure and expensive resource. In particular, we make the following **new contributions**.

- We propose **decomposing strategically selected weight matrices** across the DNN, to pinpoint a minimal set of maximally information-dense components (as observed in [47, 73, 65]) that embody the model’s IP, which must be safeguarded on the secure resource. Consequently, the remainder of the model performs most of the computations, but it becomes devoid of value and can therefore be exposed to a compromised computing resource. Since both computing resources must participate in each model inference, it incurs costs in latency and introduces new potential attacks that could exploit the communication between them.

- Thus, our paper introduces a **protocol to mitigate security risks** created by this inference hybridization. An Attacker could try to extract or approximate the valuable model information stored on the secure resource, through algebraic, denoising, or query-based attacks that exploit its clean outputs. Thus, Our protocol does not reveals clean outputs to the low-security resource, by **masking** the secure resource’s output using pre-computed noise, that can be cheaply removed later without degradation. The output is manipulated to ensure it is **uniformly distributed and independent** of the output, and thereby *perfectly secured*.

- Lastly, we provide **experimental evidence for the robustness of our approach**. We show that popular LLMs can be partitioned to create an exposed portion with most of the computations but insignificant utility, even when regions, where decomposition occurred, are bypassed. Moreover, we demonstrate that when fine-tuning the exposed portion of the model, in an attempt to restore its original performance, the recoverability is limited and can be traded off with reduced offload.

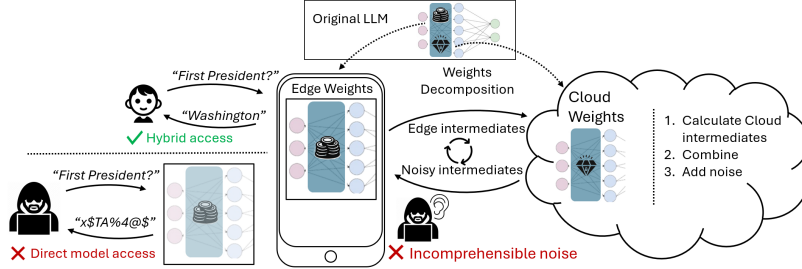


Figure 1: SLIP Framework: The figure illustrates the decomposition of the original Large Language Model between two entities: the trusted/secured party, positioned on the right, and the untrusted/non-secured edge device, on the left. During inference, the intermediary layer outputs are exchanged between these parties. The model weights stored with the secured party which embodies the model the intellectual property is safeguarded by the SLIP method, preventing theft or deduce of those weights, by tring to leverage the parties data exchanged.

1.1 Background and related works

Threat Model. In our setting, we assume an attacker is motivated to obtain the complete model parameters, i.e., its IP, for any purpose [52], while knowing the model’s architecture. To achieve the highest security guarantee in our protocol, we assume the attacker has indefinite physical access and full admin privileges in the low-security compute resource. This means this resource is adversarial, as if an attacker has take possession of it, bypassed any existing security measures, gained direct control over any exposed model parameters and can freely query the secure resource. Conversely, we assume the secure resource is a completely trusted entity, inaccessible to an attacker except through the query API. Additionally, we assume the attacker has full knowledge of our protocol and any associated hyper-parameters [55]. Thus, our protocol focuses on protecting the portion of the model assigned to the secure resource against attacks aiming to infer it, and on ensuring that the exposed model portion is devoid of any value, even after attempts to restore it through model recovery techniques [14, 45].

Model Extraction and Stealing. Model extraction attacks are a type of security threat where attackers aim to create a duplicate or approximation of a machine learning model by using its public API ([9, 64, 71, 37] see [79, 33] for review). Attackers manipulate the model’s input-output pairs to learn about its structure and functionality, allowing them to create an approximation of the model. This can enable them to use the model for their own purposes, sidestep any usage restrictions or fees, or even uncover sensitive information about the original training data. Hence, this type of attacks could compromise compute resources at any security level, whether the inference system is hybrid or not, as it exploits the intended use of the service. In contrast, model *stealing* entails unauthorized access to and replication of trained models, by circumventing the security measures [52]. Therefore, this type of attack is more likely to occur on a low-security resource involved in an hybrid inference protocol, making it the focus of our paper.

Protecting DNNs IP from Theft. Several existing methods strive to secure neural network parameters for computation on low-security resources. One approach is termed *Model Obfuscation*, the process of intentionally obscuring or hiding the critical information of a neural network while retaining its functionality. These include using knowledge distillation [75] or neural architecture search [86], intentional model poisoning [22], increasing model sensitivity to parameters perturbation [68], locating model tampering for user authorization [30] and many more [84]. However, many of these approaches degrade model accuracy, or cannot provide provable security guarantees. Additionally,

there are passive protection techniques, such as *watermarking* [72, 5, 77, 78, 81] (see [42] for survey) or *Attestation* [11], which help verify ownership and copyrights, but they cannot effectively *prevent* unauthorized access and usage to demotivate attackers. Cryptographically secure obfuscation offers provable guarantees but remains impractical for complex functions and unsuitable for scaling to even small ML models [80]. Lastly, cryptographic techniques have been extensively applied in the highly active area of Privacy Preserving Machine Learning (PPML). Such techniques include Homomorphic Encryption (e.g., [4], [53, 40]), Secure Multiparty Computation (e.g., [38, 16, 15, 44, 24]), and Differential Privacy (e.g., [2]). However, in PPML, the emphasis is on user data privacy or training data rather than protecting model weights, and existing cryptographic frameworks are not designed for this purpose, or do not account for the computational trade-offs between asymmetric parties with varying costs and security levels [61, 34, 31, 59].

2 Framework and settings

2.1 Model decomposition and properties

Here we describe a general setting for the model decomposition we suggest for offloading most of the inference computation to an untrusted entity while simultaneously protecting the model during inference. To that end, for simplicity, we denote the *trusted* entity by Charlie and the *untrusted* entity by David. For example, \mathcal{C} could be a trusted cloud or a trusted server, whereas \mathcal{D} could be an untrusted edge device or an untrusted server, or \mathcal{C} could be a trusted NPU while \mathcal{D} could be an untrusted NPU on the same server.

Definition 1 (Neural network decomposition). *Consider a model ϕ_{Θ} parameterized by Θ , and some two sets of tensors weights Θ_1 , and Θ_2 . If $\Theta = \Theta_1 \oplus \Theta_2$, where \oplus stands for the sums of tensors weights then, $(\phi_{\Theta_1}, \phi_{\Theta_2})$ is called a neural network decomposition of ϕ_{Θ} .*

Each one of the parties Charlie and David is given a different set of tensors $\Theta_{\mathcal{C}}$ and $\Theta_{\mathcal{D}}$, respectively. Thus, for simplicity, we denote the decomposition of the given model ϕ_{Θ} , by $(\phi_{\Theta_{\mathcal{C}}}, \phi_{\Theta_{\mathcal{D}}})$. We quantify the utility of a given decomposition by the following properties definitions.

Definition 2 (Neural network decomposition properties). *Consider a decomposition $(\phi_{\Theta_{\mathcal{C}}}, \phi_{\Theta_{\mathcal{D}}})$ of a given model ϕ_{Θ} parameterized by Θ . Let $P(x, y)$ be a data distribution from which the training data are sampled. Accordingly, the empirical risk of ϕ over P is given by $E_{(x,y) \sim P} [\mathcal{R}(\phi_{\Theta}(x, y))]$, where \mathcal{R} is the model loss (e.g., accuracy).*

- **Usefulness.** *Let $\phi_{\Theta^{rand}}$, be a random initialized model, parameterized by the random set of tensors Θ^{rand} . A decomposition $(\phi_{\Theta_{\mathcal{C}}}, \phi_{\Theta_{\mathcal{D}}})$ is said to be κ -effective, where κ is the true-risk ratio between the models $\phi_{\mathbf{0} \oplus \Theta_{\mathcal{D}}}$, and $\phi_{\Theta^{rand}}$, namely*

$$\kappa = E_{\Theta^{rand}} \frac{E_{(x,y) \sim P} [\mathcal{R}(\phi_{\mathbf{0} \oplus \Theta_{\mathcal{D}}}(x, y))]}{E_{(x,y) \sim P} [\mathcal{R}(\phi_{\Theta^{rand}}(x, y))]},$$

where $\mathbf{0}$ is the zeros set of tensors corresponding to $\Theta_{\mathcal{C}}$ dimensions.

- **Confidentiality.** *A decomposition $(\phi_{\Theta_{\mathcal{C}}}, \phi_{\Theta_{\mathcal{D}}})$ of ϕ_{Θ} is said to be confidential, if, for every adversary \mathcal{D}_1 , given $\Theta_{\mathcal{D}}$ and black box access to Θ , recovers ϵ_1 -approximation of the true risk of ϕ_{Θ} , namely $\epsilon_1 \cdot E_{(x,y) \sim P} [\mathcal{R}(\phi_{\Theta}(x, y))]$, (w.r.t., e.g., accuracy on a test distribution), in time T , there is adversary \mathcal{D}_2 that can construct ϵ_2 -approximation of the true risk of ϕ_{Θ} using only black box queries to Θ (i.e., without using $\Theta_{\mathcal{D}}$) for some $\epsilon_2 \approx \epsilon_1$, in time T . See Figure 2 for an illustration.*

- **Information dense.** A decomposition $(\phi_{\Theta_C}, \phi_{\Theta_D})$ is considered as η -informational densed, where $\eta = \frac{|\Theta_C|}{|\Theta|}$.

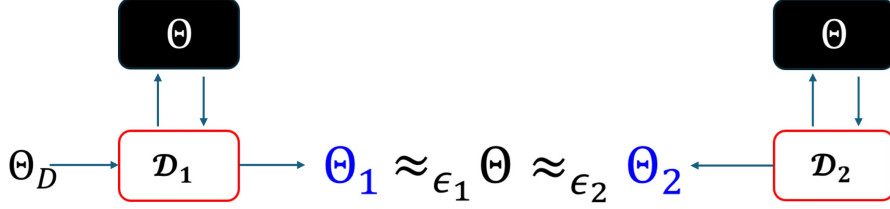


Figure 2: Confidentiality of a Model Decomposition

The Usefulness property of a decomposition implies how the exposed decomposed part of model Θ_D exhibits poor performance (e.g., random-guess accuracy). Therefore in a complementary way, it implies how well Θ_C quantifies the model’s secret IP. The more useful Θ_C is, the more secret IP is embodied in Θ_C . Accordingly, the efficiency property points out that a lower fraction of parameters $|\Theta_C|$ in \mathcal{C} implies a reduced memory space requirement and fewer operations during inference in \mathcal{C} .

2.1.1 Model decomposition via SVD

In this section, we begin by describing our decomposition method. for fully connected multilayer perceptrons (MLPs). Further, in Remark 1, we describe the generalization of this decomposition to more complex models (i.e. attention head). To decompose an MLP, we strategically identify specific critical linear layers within the network. The criteria for selecting these layers are documented in Appendix B.2. The decomposition process for these identified layers is outlined subsequently.

Let $\mathbf{W}_i \in \mathbb{R}^{d_{i+1} \times d_i}$ be the weights matrix of i -th layer, deemed critical, and where $d_i, d_{i+1} \in \mathbb{N}$ are the widths of the i -th and $(i + 1)$ -st layers, respectively. To avoid cluttering notation, we will omit the subscript in what follows and denote $m := d_{i+1}$ and $n := d_i$. Singular Value Decomposition (SVD) of \mathbf{W} is given by $\mathbf{W} = \mathbf{U}\Sigma\mathbf{V}^\top = \sum_{j=1}^r \sigma_j \mathbf{u}_j \mathbf{v}_j^\top$, where, $\text{rank}(\mathbf{W}) =: r \leq \min\{m, n\}$, $\Sigma = \text{diag}(\sigma_1, \dots, \sigma_r)$ is a rectangular diagonal matrix with σ_j the j -th singular value of \mathbf{W} , and $\{\mathbf{u}_j \in \mathbb{R}^m\}_{j \in [m]}$ and $\{\mathbf{v}_j \in \mathbb{R}^n\}_{j \in [n]}$ are left and right (resply.) singular vectors of \mathbf{W} .

We then define, \mathbf{W}^C – the sensitive part to be held by \mathcal{C} – to be the part of \mathbf{W} defined by its top k singular components, where $1 < k \ll \text{rank}(\mathbf{W})$ is a parameter we call the *sensitivity rank* (that depends on the model and the layer). The remaining part \mathbf{W}^D of \mathbf{W} is offloaded to the untrusted entity \mathcal{D} . More precisely,

$$\mathbf{W}^C = \sum_{j=1}^k \sigma_j \mathbf{u}_j \mathbf{v}_j^\top \quad \text{and} \quad \mathbf{W}^D = \sum_{j=k+1}^n \sigma_j \mathbf{u}_j \mathbf{v}_j^\top. \quad (1)$$

In the notation of the previous subsection, the decomposition $(\text{MLP}_{\Theta_C}, \text{MLP}_{\Theta_D})$ for an MLP_Θ is then defined as follows. For each critical layer of Θ , apply (1) to its weight matrix \mathbf{W} and include the matrix \mathbf{W}^C and the next nonlinear layer (such as Relu) in Θ_C and include \mathbf{W}^D in Θ_D . For each non-critical layer of include the entire weight matrix and the next nonlinear layer in Θ_D (without adding anything to \mathcal{D}).

The following insights imply that the suggested technique for model decomposition is optimal, namely, simultaneously holding both the effectiveness and the efficiency properties.

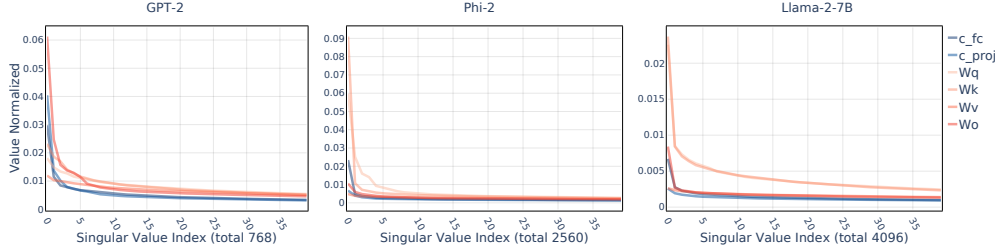


Figure 3: Singular values of the weight matrices of each model, sorted from largest to smallest.

Information decay. Intuition for the decomposition in (1) comes from the plots in Figure 3. They show that several popular models exhibit an exponential decay of their singular values for important linear layers. To the extent that singular components capture the distribution of “essential information” of a weight matrix – a claim that we will further justify in Section 4 – this shows that a value $k \ll \text{rank}(\mathbf{W})$ can be chosen and weight matrix \mathbf{W} can be split as in (1) so that much of the “secret” information is retained in $\mathbf{W}^{\mathcal{C}}$ by \mathcal{C} . We consider any suitable $k > 1$ since in Appendix E.0.1 we show an attack that proves that if \mathcal{C} holds just the top singular component $k = 1$ of \mathbf{W} and offloads the rest of \mathbf{W} to an untrusted \mathcal{D} , then \mathcal{D} can extract $\mathbf{W}^{\mathcal{C}}$ by solving a system of linear equations formed from a small number of inference queries.

2.2 Securing protocol framework

In the real world, to secure the two parties \mathcal{C} and \mathcal{D} run an interactive protocol Π to run inference on ϕ_{Θ} . At the beginning of the protocol, Π , \mathcal{C} and \mathcal{D} both receive the input x , and at the end of executing Π , they should both obtain the output of the protocol $\Pi(x)$, which must be equal $\phi_{\Theta}(x)$. Even after several executions of Π , \mathcal{D} should not be able to learn \mathcal{C} ’s part $\Theta_{\mathcal{C}}$.¹

We elaborate on the last two points above with the informal definitions below to help quantify the utility of such decompositions.

Definition 3 (Efficiency). *For a protocol Π as described above, let $T_{\Theta}(\Pi)$ be time complexity computation of the model under the protocol. Analogously, let $T_{\Theta_{\mathcal{C}}}(\Pi)$, and $T_{\Theta_{\mathcal{D}}}(\Pi)$ be the time complexity computation of local computation of \mathcal{C} and \mathcal{D} , respectively. A decomposition $(\phi_{\Theta_{\mathcal{C}}}, \phi_{\Theta_{\mathcal{D}}})$ of ϕ_{Θ} is said to be ϵ -efficient if there is for a protocol Π such that, for a small $\epsilon > 0$,*

$$T_{\Theta_{\mathcal{C}}}(\Pi) \leq \epsilon \cdot T_{\Theta}(\Pi). \quad (2)$$

Definition 4 (Safety). *A decomposition $(\phi_{\Theta_{\mathcal{C}}}, \phi_{\Theta_{\mathcal{D}}})$ of ϕ_{Θ} is called safe if an associated protocol Π exists such that Π is both efficient and confidential.*

The main hypothesis we put forth in this paper is that all LLMs have safe decompositions. We give supporting empirical and theoretical evidence to support this hypothesis. Specifically, this is done by applying Singular Value Decomposition on certain critical layers of the model to split a model between a trusted entity and an untrusted entity. We then use cryptographic protocols that are safe: they can provably, under cryptographic assumptions, resist a *natural reconstruction strategy* by an adversarial untrusted entity that tries to recover the trusted part of the model layer by layer. There are tradeoffs between the efficiency protocols and strength of guarantees against this class of

¹More generally, we could insist that \mathcal{D} not be able to learn a functionally (even approximately) equivalent model to Θ except by essentially training such a model from scratch.

attacks giving a spectrum of choices for the protocols. Protecting against arbitrary reconstruction attacks by an adversarial \mathcal{D} appears to be a long term research challenge.

3 Hybrid inference protocol

In this section, we introduce a protocol designed to secure the decomposed two MLP sequential weights $\mathbf{W}_i^{\mathcal{C}}$ and $\mathbf{W}_{i+1}^{\mathcal{C}}$, which constitute critical intellectual property (IP) of the model, against theft by an attacker with access to an edge device. Simply utilizing singular value decomposition (SVD) to split the layers does not adequately protect against potential threats, as attackers might still deduce the hidden components of the weights using methods such as denoising, query-based attacks, algebraic techniques, or model recovery strategies. We demonstrate that the proposed protocol perfectly secures against these attacks. Furthermore, in Section 4, we illustrate that applying this protocol to (only a few) select sequential layers can adequately secure the model IP.

Additionally, for the validity and practicality of the following operations and claims, we consider all parameters to be integers with general precision denoted by q (i.e Int8, Int32), such that $\mathbf{W}_i, \mathbf{W}_{i+1} \in \mathbb{Z}_q^{d_{i+1} \times d_i}$. Typically, widely employed quantization techniques convert floating-point weights into an integer format; accordingly, our method is also applicable. It is important to note that deployed neural networks in real-world scenarios often operate using low-precision weights. Therefore, we evaluate our solution under these conditions.

Pre-deployment noise generation. Ahead of the model deployment, where the model is stored only on the \mathcal{C} , it generates a large batch of *i.i.d* random vectors (i.e much larger than the dimension of the model layers $\sim N = 2^{32}$) per any layer on which the protocol would be applied, that are the size of the layer input. Those vectors will serve later, in inference time, to generate the noise that will be required to mask outputs from \mathcal{C} to \mathcal{D} . These vectors will be periodically refreshed according to the used protocol and required security level, where in the basic protocol each random vector will be used only once. We denote these vectors by $\mathbf{z}_{1,i}, \mathbf{z}_{2,i}, \dots, \mathbf{z}_{N,i} \sim \text{Uniform}[0, L]^{d_i}$, where we assume that $\mathbf{Z}_i \mathbf{Z}_i^{\top} \in \mathbb{Z}_q^{d_i \times d_i}$ is of full rank (the noise lies on full dimension field), and $L \in \mathbb{Z}_q$ is a predefined number (to be chosen according to the numbers ranges in the problem, namely the data, and weight values). The \mathcal{C} shell keeps those vectors in its storage, but not in its memory (for efficient memory consumption). In addition, any multiplication $\forall [i, j], \mathbf{W}_i^{\mathcal{D}} \mathbf{z}_{j,i}$ is computed in advance and stored in the \mathcal{C} storage, as well, this will be an essential tool in the method being used to cancel the propagated noise. For clarity, we denote $\tilde{\mathbf{z}}_{j,i} = \mathbf{W}_i^{\mathcal{D}} \mathbf{z}_{j,i}$. In subsection 3.3 we suggest a costly-efficient sophisticated alternative version.

Remark 1. *For clarity, without loss of generality, our approach is applied to MLP layers. However, the methods apply to other models that include linear operators. For example, convolution layers can be represented as a linear operator with a restricted weights structure matrix. As an additional example, a detailed description of the protocol for the attention head layer appears in Appendix ??.*

3.1 Protocol overview

In this subsection, we present an overview of the protocol, as described in Figure 4, and subsequently, in Subsection 3.2, we establish the correctness of the protocol and demonstrate its capability to secure data under reasonable assumptions. This protocol is designed to ensure the security of hybrid inference processes involving two consecutive layers of indexes i and $i + 1$, within the range $[1, m]$, where m represents the total number of layers in the model. For a given inference prompt \mathbf{x} , the input is the output activation a_{i-1} from the preceding layer. Notably, if $i = 1$, the protocol input

$\mathbf{a}_0 = \mathbf{x}_t$ which is the initial input to the model. The protocol has three stages in layer i and two in layer $i+1$. The protocol unfolds as follows.

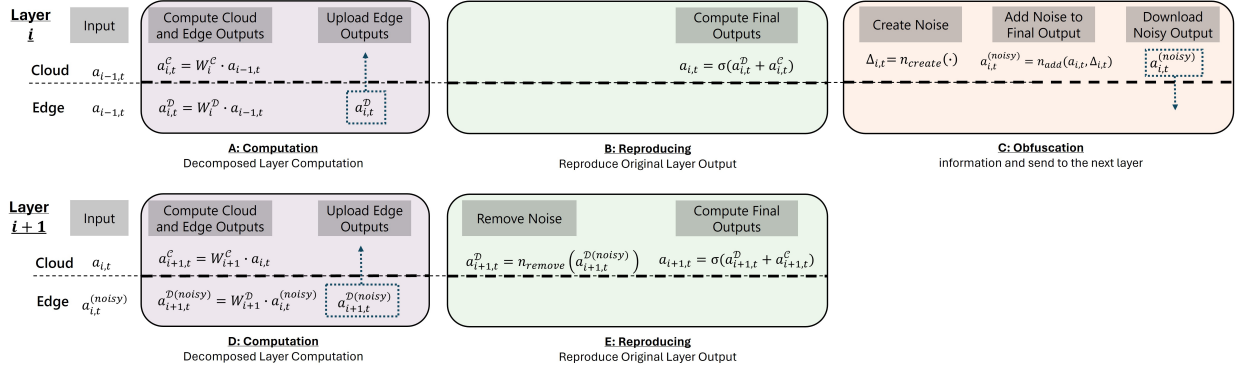


Figure 4: Efficient and perfectly secured protocol for hybrid inference

- **A- Computation:** parallelly \mathcal{D} and \mathcal{C} compute their cross-product of the respective *decomposed weight matrix* with the input, namely $\mathbf{a}_i^{\mathcal{D}} = \mathbf{W}_i^{\mathcal{D}} \mathbf{a}_{i-1}$, and $\mathbf{a}_i^{\mathcal{C}} = \mathbf{W}_i^{\mathcal{C}} \mathbf{a}_{i-1}$. Then \mathcal{D} sends its result, the vector $\mathbf{a}_i^{\mathcal{D}}$ to \mathcal{C} .

- **B- Reproducing:** \mathcal{C} combines both products of the previous stage, to get the original i 's layer output, the one that would be calculated under regular non-decomposed model inference (one-party setting). It obtained by simply applies the activation function σ on the sum of both terms: $\mathbf{a}_i = \sigma(\mathbf{a}_i^{\mathcal{C}} + \mathbf{a}_i^{\mathcal{D}}) = \sigma((\mathbf{W}_i^{\mathcal{C}} + \mathbf{W}_i^{\mathcal{D}}) \mathbf{a}_{i-1}) = \sigma(\mathbf{W}_i \mathbf{a}_{i-1})$. The activation output \mathbf{a}_i indeed could be the input to the next layer $i+1$, however, it embodies an analytical relation to $\mathbf{W}_i^{\mathcal{C}}$, a fact that could leveraged to infer the layer's secret, and therefore it could not be sent and shared with \mathcal{D} as-is, and must be securely masked before.

- **C- Obfuscation:** \mathcal{C} is masking the activation \mathbf{a}_i as follows, it first create the noise $\Delta_i = n_{create}(\cdot)$, where $n_{create}(\cdot)$ is a noise creation function that can be implemented in several ways. Then it combines the noise with the activation to get $\mathbf{a}_i^{(noisy)} = n_{add}(\mathbf{a}_i, \Delta_i)$, where $n_{add}(\cdot)$ is a dedicated function for that purpose and $\mathbf{a}_i^{(noisy)}$ is the noisy activation that can be securely downloaded to \mathcal{D} . In our case we implemented these functions as follows:

$$\mathbf{a}_i^{(noisy)} = n_{add}(\mathbf{a}_i, \Delta_i) \triangleq \text{mod}(\mathbf{a}_i + \Delta_i, L),^2 \quad (3)$$

$$\Delta_i = n_{create}(\cdot) \triangleq \mathbf{z}_i \quad (4)$$

In subsection 3.3 we provide generalized version for Δ_i . Layer $i+1$ of the protocol has an additional 2 stages:

- **D- Computation:** this is exactly the same as stage **A** but now with the noisy input $\mathbf{a}_i^{(noisy)}$ which is the output of stage **C** from the previous layer i . Therefore the output will be $\mathbf{a}_{i+1}^{\mathcal{D}(noisy)} = \mathbf{W}_{i+1}^{\mathcal{D}} \mathbf{a}_i^{(noisy)}$. Then \mathcal{D} send it back to \mathcal{C} .

- **E- Reproducing:** \mathcal{C} first removing the noise from $\mathbf{a}_{i+1}^{\mathcal{D}(noisy)}$ by applying a dedicated noise removal function $\mathbf{a}_{i+1}^{\mathcal{D}} = n_{remove}(\mathbf{a}_{i+1}^{\mathcal{D}(noisy)})$, and now it holds two "clean" decomposed weight matrices $\mathbf{a}_{i+1}^{\mathcal{C}}$ and $\mathbf{a}_{i+1}^{\mathcal{D}}$ so it can calculate the \mathbf{a}_{i+1} layer's output same as in stage **B**.

In our case we implemented the noise removal function based on lemma 1, by applying

$$\mathbf{a}_{i+1}^{\mathcal{D}} = n_{remove}(\mathbf{a}_{i+1}^{\mathcal{D}(noisy)}) \triangleq \text{mod}(\mathbf{a}_{i+1}^{\mathcal{D}(noisy)} - \tilde{\Delta}_i, L). \quad (5)$$

² $\mathbf{a}_i^{(noisy)} \sim \mathbf{U}[0, L]$ by Lemma 2, implying that the device learn nothing about the \mathcal{C} weights.

In case the next layer ($i+2^{th}$) is also decomposed, the protocol will continue to stage **C:Obfuscation** by adding mask noise to the resulting activation \mathbf{a}_{i+1} of the current $i+1^{th}$ layer.

3.2 Theoretical guarantees

The following lemma shows the effective removal of the noise propagated at E:Reproducing 3.1.

Lemma 1. *The noise reduction equation 5 satisfies*

$$\text{mod}(\mathbf{W}_{i+1}^{\mathcal{D}} \mathbf{a}_i, L) = \text{mod}(\mathbf{a}_{i+1}^{\mathcal{D}(\text{noisy})} - \tilde{\Delta}_i, L),$$

namely, if the original result fits L , $\|\mathbf{W}_{i+1}^{\mathcal{D}} \mathbf{a}_i\|_{\infty} < L$, then $\mathbf{a}_{i+1}^{\mathcal{D}} = \mathbf{W}_{i+1}^{\mathcal{D}} \mathbf{a}_i$.

The outcome of the noise cancellation on \mathcal{D} is equivalent to the results that would be achieved in the absence of noise masking (assuming it fits L). Consequently, the performance in the \mathcal{C} is comparable to that in a single-party setup, without any degradation in accuracy.

Hypothetically, sending activation \mathbf{a}_i to \mathcal{D} by the \mathcal{C} would result in exposing the secret decomposed weights to \mathcal{D} . Indeed, given a strong analytical relation between the activation and the \mathcal{C} decomposed weights, the adversary may be able to reconstruct the layer’s weights. The following lemma shows that the proposed masking algorithm perfectly secures the activation, which in turns ensure perfect protection of the decomposed layer’s weights.

Theorem 2 (Perfectly secure masking). *Given a discrete random variable $s \in \mathbb{Z}^d$ and random noise $n \sim \mathbf{U}[0, L - 1]^d$, we define a masked variable as $s_n = \text{mod}(s + n, L)$. Then $s_n \sim \mathbf{U}[0, L - 1]^d$, and s_n and s are independent, namely the masking is perfectly secured.*

A visual illustration of the making effect is given in the following Figure .

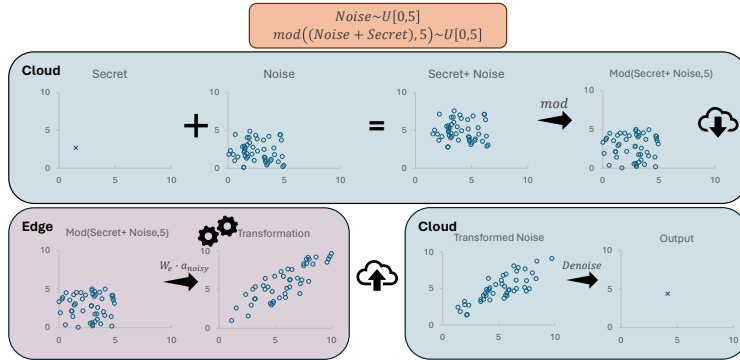


Figure 5: Efficient and perfectly masking a given secret.

Example 1 (Non-feasible inference-averaging attack). *Consider a sophisticated attacker, exposed to \mathcal{D} enters the LLM in the same inference batch, denoted by \mathbf{x} . Therefore, in the i -th layer, an intermediate inference $\mathbf{a}_i + \Delta_i$ will be obtained. Still, we will remember that the masking would result in $\text{mod}(\mathbf{a}_i + \Delta_i, L)$. Therefore it will not be possible to minimize (almost nullifying) the masking that is allegedly expressed by noising the true signal, so that the clean signal, namely \mathbf{a}_i , will be revealed and so the decomposed weights of The i -th layer would be exposed.*

3.3 Masking generalization: cost efficient

The computation of noise cancellation vectors $\tilde{\mathbf{z}}_{t,i}$ might be costly; therefore, to decrease the operational expenses associated with preparing these vectors in the background, several enhancements are suggested herein. Remember that generating the vectors $\tilde{\mathbf{z}}_{t,i}$ necessitates storing the decomposed \mathbf{W}_i^D in the \mathcal{C} and computing $\tilde{\mathbf{z}}_{t,i} = \mathbf{W}_i^D \mathbf{z}_{t,i}$. This process is for new vectors $\mathbf{z}_{t,i}$ that are continually regenerated in the background to augment the pre-existing, extensive set of random vectors created prior to deployment. The most straightforward extension would be to use the $\mathbf{z}_{j,i}$ from the pre-existing set of vectors and the corresponding $\tilde{\mathbf{z}}_{j,i}$ multiple time, where the index j will be selected in random.

Initially, to reduce the seemingly risk that an adversary would be able to learn the available noise vectors in \mathbf{Z}_i by sampling it multiple times, the pre-computed batch size N of \mathbf{Z}_i should be selected to be a large enough (e.g., $N > 10e6$) along with a limited number (e.g., 2) the same vector $\mathbf{z}_{j,i}$ can be re-used. In principal, to mitigate the aforementioned risk, a linear combination of a small number ℓ of randomly selected noise vectors from \mathbf{Z}_i will be used instead of a single vector from \mathbf{Z}_i

$$\Delta_i = \text{mod}\left(\sum_{j \in S_i} \alpha_j \mathbf{z}_{j,i}, L\right),$$

where S_i is a set of size ℓ of random indexes $[1, N]$, $\alpha_j \in \mathbb{Z}_L$ are co-prime scalars with L randomly generated in inference time t (real-time) . The resulting Δ_i still $\mathbf{U}[0, L - 1]$ as shown in Lemma 3.

Lemma 3. *Given $n_i \sim \mathbf{U}[0, L - 1]^d$ and $\alpha_i \in \mathbb{Z}_L$ co-prime to L for $i = 1..l$, $n_s = \text{mod}(\sum_{i=1}^l \alpha_i n_i, L)$ is distributed $\mathbf{U}[0, L - 1]^d$.*

The corresponding noise cancellation vector is computed as following $\tilde{\Delta}_i = \sum_{j \in S_i} \alpha_j \tilde{\mathbf{z}}_{j,i}$. The computation of Δ_i and $\tilde{\Delta}_i$ requires only $O(\ell d_i)$ operation using ℓ pre-computed $\mathbf{Z}_i \in \mathbb{Z}^{d_i}$ selected in S_i . The conditions of Lemma 1 still holds, so the same equation 5 is used to cancel the noise. The advantage of this extension is ensuring that the chance to get $S_{i,t_1} = S_{i,t_2}$ for $t_2 > t_1$ is negligible.

Example 2. *for $N = 10^6$ and $l = 50$, there are $\sim 10^{235}$ possible distinct combinations of $\mathbf{z}_{j,i}$, so the chance to get the same combination at least twice after 10^{15} trials is $\sim 10^{-206}$, which make it practically impossible, these even without taking in account an additional randomization provided by α_j . Please refer to appendix D to a detailed analysis.*

4 Experiments

Experimental Setup. In this section, we explore how to obtain a neural network decomposition with the desired properties. This is examined through benchmarking various decompositions with the WikiText dataset [48] and assessing their effectiveness against fine-tuning attacks. We conducted tests on LLaMA2-7B [70], Phi-2 [49], and GPT-2 Small [58], using EleutherAI’s evaluation code [19] to measure perplexity on a word completion task, where higher scores indicate lower performance. We used NVIDIA A100 GPU for all of our experiments.

Decomposition effectiveness. We aimed to show it is possible to decompose a model into a small, secured and information-rich portion and a large, exposed and valueless portion that is devoid of IP. Thus, for each of the three models, we evaluated multiple distinct decompositions, each defined by choosing a specific decoder block and a particular layer type within the block (MLP layers (c_fc , c_proj) or attention layers ($\mathbf{W}_q, \mathbf{W}_k, \mathbf{W}_v, \mathbf{W}_o$), and a specific number of singular values to remove from the layer’s weight matrix. Each decomposition is represented by a single dot in the

Algorithm 1 Sequential Masking Protocol Via Random Stream

Input: Previous layer output \mathbf{a}_{i-1} ; Inference number t ; Two decomposed sequential layers $\mathbf{W}_i \in \mathbb{R}^{d_{i+1} \times d_i}$, and $\mathbf{W}_{i+1} \in \mathbb{R}^{d_{i+2} \times d_{i+1}}$; pre-computed random noise $\mathbf{z}_{1,i}, \mathbf{z}_{2,i}, \dots, \mathbf{z}_{N,i}$, and their corresponding $\tilde{\mathbf{z}}_{1,i}, \tilde{\mathbf{z}}_{2,i}, \dots, \tilde{\mathbf{z}}_{N,i}$; (Optional) Masking matrices $\mathbf{R}_i, \mathbf{R}_{i+1}$.

Parallel compute of \mathcal{D} and \mathcal{C} Parties:

<p>The \mathcal{D} party: $\mathbf{a}_i^{\mathcal{D}} \leftarrow \mathbf{W}_i^{\mathcal{D}} \mathbf{a}_{i-1}$</p>	<p>The \mathcal{C} party: $\mathbf{a}_i^{\mathcal{C}} \leftarrow \mathbf{W}_i^{\mathcal{C}} \mathbf{a}_{i-1}$ $S_i \leftarrow \text{UniformSample}(\{1, 2, \dots, N\}, \ell)$ $\Delta_i \leftarrow \sum_{j \in S_i} \alpha_j \mathbf{z}_{j,i}$ $\mathbf{a}_i^{(\text{noisy})} \leftarrow \mathbf{a}_i + \Delta_i.$</p>
<p>\mathcal{D} computes: $\mathbf{a}_{i+1}^{\mathcal{D}(\text{noisy})} \leftarrow \mathbf{W}_{i+1}^{\mathcal{D}} \mathbf{a}_i^{(\text{noisy})}$ $\{\equiv \mathbf{a}_{i+1}^{\mathcal{D}} + \sum_{j \in S_i} \alpha_j \tilde{\mathbf{z}}_{j,i}\}$</p> <p>$\mathcal{D}$ sends $\mathbf{a}_{i+1}^{\mathcal{D}(\text{noisy})}$ to \mathcal{C}</p> <p>\mathcal{C} compute $n_i \leftarrow \sum_{j \in S_i} \alpha_j \tilde{\mathbf{z}}_{j,i}$ $\{\text{propagated noise}\}$</p> <p>$\mathcal{C}$ compute $\mathbf{a}_{i+1} \leftarrow \sigma \left(\mathbf{a}_{i+1}^{\mathcal{C}} + \mathbf{a}_{i+1}^{\mathcal{D}(\text{noisy})} - n_i \right)$ $\{\equiv \sigma \left(\mathbf{a}_{i+1}^{\mathcal{C}} + \mathbf{a}_{i+1}^{\mathcal{D}} \right)\}$</p> <p>Return \mathbf{a}_{i+1}.</p>	

figure, representing an almost full LLM, missing only a number of singular values (indicated on the x axis), in a single layer (indicated by the trace) and a single block. To emphasise the effectiveness between layer types only, we averaged the results across all the blocks of an LLM for the same layer type. Results in figure 6 show that for each model examined, there are at least a few layer types from which removing even a small amount of singular vectors (< 10) in a single block can significantly degrade model perplexity. Model scores plummeted from a baseline perplexity of around 10 to thousands, indicating that these vectors hold significant IP.

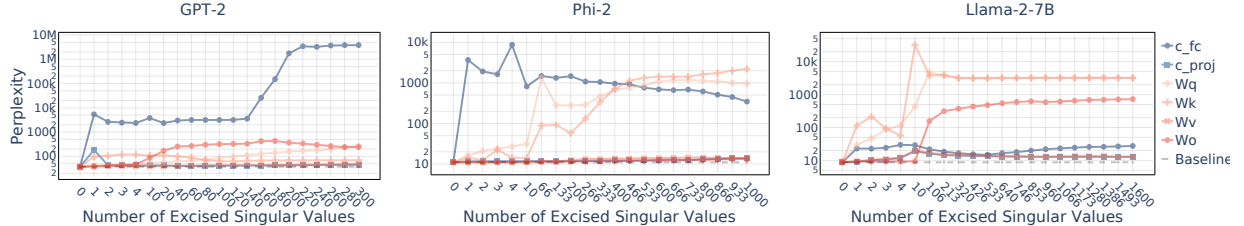


Figure 6: Perplexity scores for all three models, after removing various numbers of singular values from different layer types in a single decoder block. Results are averaged across all possible blocks.

Block effectiveness. We explored the impact of bypassing different sequences of decoder blocks on the effectiveness of an exposed model, to identify optimal blocks for decomposition. Testing the three LLMs, we bypassed 1, 3, 5, or 7 consecutive blocks and recorded the subsequent perplexity (see figure 7). Bypassing early blocks severely degraded performance, indicating they hold substantial IP and are crucial for decomposition. This is consistent with findings [23] that show shallow blocks are vital for knowledge retention. Bypassing the last blocks also reduced performance, but less so.

Exposed Model recovery. We investigated the consequences of fine-tuning [25] using public datasets to restore the compromised portion of the phi-2 model. Using the Alpaca dataset [69] and LoRA [29], we fine-tuned for 10 epochs across five decomposition configurations and one with randomized model parameters. Each configuration is characterized by an index (1-6), percentage

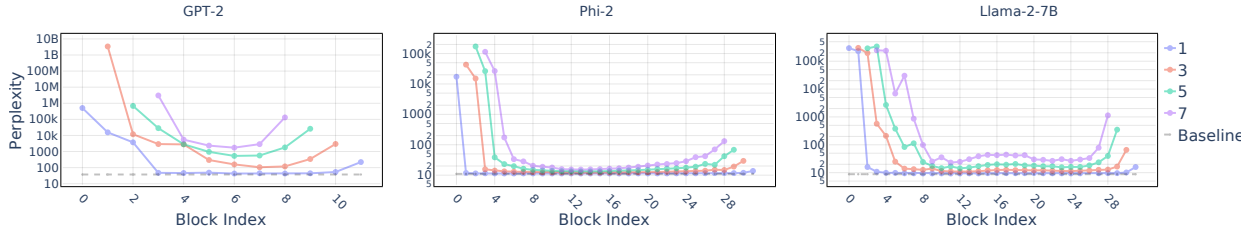


Figure 7: Performance degradation of the LLMs when bypassing windows of 1, 3, 5, or 7 consecutive blocks. The x-axis represents the center block of each window, while the y-axis shows the perplexity.

of offload (calculated as defined by the efficiency property), and amount of excised singular values, and the number of blocks in which all layer types were decomposed at the beginning (+) and end (-) of the model. After decomposition, all exposed models showed random performance, but after fine-tuning we observed that as less computation is offloaded and more of the model is exposed, recovery becomes easier. Configurations offloading 92% to 97.5% remained robust against recovery, as depicted in figure 8.

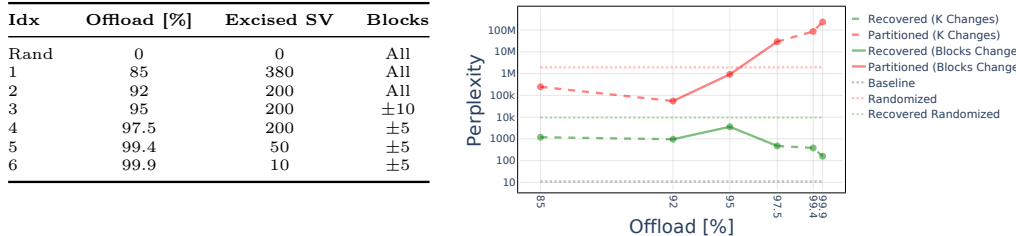


Figure 8: Impact of fine-tuning on various decomposition configurations, detailed in the left table.

Compute & latency analysis. We simulated the latency of a neural network decomposition between an edge device and a cloud server, considering the computational capacities of GPUs, network bandwidth and delay. Our simplified analysis, based on a version of Llama2 [70] with only feed-forward layers, decomposed in a third of its layers, shows edge computation dominates latency (150.34 ms), followed by data transfer (71.31 ms), with cloud computation being minimal (0.66 ms). Our approach leaves a mere 1.5% of operations to the cloud (see details in C).

5 Discussion

In this paper, we presented SLIP, a novel hybrid inference technique designed to safeguard DNNs, especially LLMs, against theft when offloaded to low-security resources like edge devices, leaving minimal computations on the secure resource, such as the cloud or trusted execution environments. To our knowledge, SLIP is the first such technique that is both practical for real-world use and provably secure, without compromising model accuracy or introducing significant latency. The technique’s security is multifaceted: it leverages the rapid decay of singular values in LLM weight matrices to effectively decompose them and store only the most critical singular vectors securely, while the remaining model is useless and robust against restoration attempts with fine-tuning. The secret model is protected from an adversarial compute resource through our secure inference protocol, which is provably secure and efficient. Practically, SLIP introduces minimal computational

overhead at inference, with latency primarily influenced by network delays, which can be mitigated in scenarios with ample bandwidth, such as when using a TEE. Additionally, the technique does not cause degradation in accuracy since decomposition retrains the original results, and the noise added is canceled completely. These properties make SLIP highly promising for industry application, enabling cost-effective model deployment on edge devices, and providing a foundation for the research community to enhance security and efficiency in a hybrid inference framework.

Limitations & Future Work. Our protocol’s current limitations present opportunities for further research, including testing on additional models and tasks, and quantifying latency and FLOPs in practical implementations. Additionally, future work could focus on developing algorithms to efficiently determine the optimal model decomposition that balances security, latency, and offload according to the model owner’s preferences. Moreover, this framework can be expanded to secure user prompts for privacy, obfuscate model architecture, and enhance the efficiency of noise generation, retrieval, and removal processes.

References

- [1] A. Anonymous. Crayon: Customized on-device llm via instant adapter blending and edge-server hybrid inference. *ACL 2024*, Under Review. Paper under review.
- [2] M. Abadi, A. Chu, I. Goodfellow, H. B. McMahan, I. Mironov, K. Talwar, and L. Zhang. Deep learning with differential privacy. In *Proceedings of the 2016 ACM SIGSAC conference on computer and communications security*, pages 308–318, 2016.
- [3] M. Abdalla, F. Bourse, A. De Caro, and D. Pointcheval. Simple functional encryption schemes for inner products. In *IACR International Workshop on Public Key Cryptography*, pages 733–751. Springer, 2015.
- [4] A. Acar, H. Aksu, A. S. Uluagac, and M. Conti. A survey on homomorphic encryption schemes: Theory and implementation. *ACM Computing Surveys (Csur)*, 51(4):1–35, 2018.
- [5] Y. Adi, C. Baum, M. Cisse, B. Pinkas, and J. Keshet. Turning your weakness into a strength: Watermarking deep neural networks by backdooring. In *27th USENIX Security Symposium (USENIX Security 18)*, pages 1615–1631, 2018.
- [6] A. Beimel. Secret-sharing schemes: A survey. In *International conference on coding and cryptology*, pages 11–46. Springer, 2011.
- [7] Y. Bengio and Y. LeCun. Scaling learning algorithms towards AI. In *Large Scale Kernel Machines*. MIT Press, 2007.
- [8] Y. Bengio and Y. LeCun. Scaling learning algorithms towards AI. In *Large Scale Kernel Machines*. MIT Press, 2007.
- [9] L. Birch, W. Hackett, S. Trawicki, N. Suri, and P. Garraghan. Model leeching: An extraction attack targeting llms, 2023.
- [10] G. Chaopeng, L. Zhengqing, and S. Jie. A privacy protection approach in edge-computing based on maximized dnn partition strategy with energy saving. *Journal of Cloud Computing*, 12(1):29, 2023.
- [11] H. Chen, C. Fu, B. D. Rouhani, J. Zhao, and F. Koushanfar. Deepattest: An end-to-end attestation framework for deep neural networks. In *Proceedings of the 46th International Symposium on Computer Architecture*, pages 487–498, 2019.
- [12] J. Chen and X. Ran. Deep learning with edge computing: A review. *Proceedings of the IEEE*, 107(8):1655–1674, 2019.
- [13] M. Chen and M. Wu. Protect your deep neural networks from piracy. *IEEE Transactions on Computer-Aided Design of Integrated Circuits and Systems*, pages 1–7, 2020.
- [14] T. Chen, T. Ding, B. Yadav, I. Zharkov, and L. Liang. Lorashear: Efficient large language model structured pruning and knowledge recovery, 2023.
- [15] K. Cheng, N. Xi, X. Liu, X. Zhu, H. Gao, Z. Zhang, and Y. Shen. Private inference for deep neural networks: A secure, adaptive, and efficient realization. *IEEE Transactions on Computers*, 72(12):3519–3531, 2023.

- [16] A. Dalskov, D. Escudero, and M. Keller. Secure evaluation of quantized neural networks. *Proceedings on Privacy Enhancing Technologies*, 2020(4):355–375, Aug. 2020.
- [17] D. Ding, A. Mallick, C. Wang, R. Sim, S. Mukherjee, V. Ruhle, L. V. S. Lakshmanan, and A. H. Awadallah. Hybrid llm: Cost-efficient and quality-aware query routing, 2024.
- [18] L. Fan, K. Ng, and C. S. Chan. Rethinking deep neural network ownership verification: Embedding passports to defeat ambiguity attacks. In *Proceedings of the Annual Conference on Neural Information Processing Systems*, pages 4716–4725, 2019.
- [19] L. Gao, J. Tow, B. Abbasi, S. Biderman, S. Black, A. DiPofi, C. Foster, L. Golding, J. Hsu, A. Le Noac’h, H. Li, K. McDonell, N. Muennighoff, C. Ociepa, J. Phang, L. Reynolds, H. Schoelkopf, A. Skowron, L. Sutawika, E. Tang, A. Thite, B. Wang, K. Wang, and A. Zou. A framework for few-shot language model evaluation, 12 2023.
- [20] I. Goodfellow, Y. Bengio, and A. Courville. *Deep Learning*, volume 1. MIT Press, 2016.
- [21] I. Goodfellow, Y. Bengio, A. Courville, and Y. Bengio. *Deep learning*, volume 1. MIT Press, 2016.
- [22] M. Grailoo, Z. U. Abideen, M. Leier, and S. Pagliarini. Preventing distillation-based attacks on neural network ip, 2022.
- [23] A. Gromov, K. Tirumala, H. Shapourian, P. Glorioso, and D. A. Roberts. The unreasonable ineffectiveness of the deeper layers, 2024.
- [24] K. Gupta, N. Jawalkar, A. Mukherjee, N. Chandran, D. Gupta, A. Panwar, and R. Sharma. Sigma: Secure gpt inference with function secret sharing. Cryptology ePrint Archive, Paper 2023/1269, 2023. <https://eprint.iacr.org/2023/1269>.
- [25] Z. Han, C. Gao, J. Liu, S. Q. Zhang, et al. Parameter-efficient fine-tuning for large models: A comprehensive survey. *arXiv preprint arXiv:2403.14608*, 2024.
- [26] G. E. Hinton, S. Osindero, and Y. W. Teh. A fast learning algorithm for deep belief nets. *Neural Computation*, 18:1527–1554, 2006.
- [27] G. E. Hinton, S. Osindero, and Y. W. Teh. A fast learning algorithm for deep belief nets. *Neural Computation*, 18:1527–1554, 2006.
- [28] X. Hou, J. Liu, J. Li, Y. Li, W. jie Lu, C. Hong, and K. Ren. Ciphergpt: Secure two-party gpt inference. Cryptology ePrint Archive, Paper 2023/1147, 2023.
- [29] E. J. Hu, Y. Shen, P. Wallis, Z. Allen-Zhu, Y. Li, S. Wang, L. Wang, and W. Chen. Lora: Low-rank adaptation of large language models, 2021.
- [30] L. Huang, G. Zhao, and C. Qin. Recoverable active protection framework for neural network models. In *2023 IEEE International Workshop on Information Forensics and Security (WIFS)*, pages 1–6, 2023.
- [31] Z. Huang, W.-j. Lu, C. Hong, and J. Ding. Cheetah: Lean and fast secure {Two-Party} deep neural network inference. In *31st USENIX Security Symposium (USENIX Security 22)*, pages 809–826, 2022.

- [32] T. Ishiyama, T. Suzuki, and H. Yamana. Highly accurate cnn inference using approximate activation functions over homomorphic encryption. In *2020 IEEE International Conference on Big Data (Big Data)*, pages 3989–3995. IEEE, 2020.
- [33] M. Jagielski, N. Carlini, D. Berthelot, A. Kurakin, and N. Papernot. High accuracy and high fidelity extraction of neural networks. In *29th USENIX security symposium (USENIX Security 20)*, pages 1345–1362, 2020.
- [34] C. Juvekar, V. Vaikuntanathan, and A. Chandrakasan. {GAZELLE}: A low latency framework for secure neural network inference. In *27th USENIX security symposium (USENIX security 18)*, pages 1651–1669, 2018.
- [35] Y. Kang, J. Hauswald, C. Gao, A. Rovinski, T. Mudge, J. Mars, and L. Tang. Neurosurgeon: Collaborative intelligence between the cloud and mobile edge. In *Proceedings of the Twenty-Second International Conference on Architectural Support for Programming Languages and Operating Systems, ASPLOS '17*, page 615–629, New York, NY, USA, 2017. Association for Computing Machinery.
- [36] Y. Kang, J. Hauswald, C. Gao, A. Rovinski, T. Mudge, J. Mars, and L. Tang. Neurosurgeon: Collaborative intelligence between the cloud and mobile edge. *SIGARCH Comput. Archit. News*, 45(1):615–629, apr 2017.
- [37] S. Kariyappa, A. Prakash, and M. K. Qureshi. Maze: Data-free model stealing attack using zeroth-order gradient estimation. In *Proceedings of the IEEE/CVF Conference on Computer Vision and Pattern Recognition (CVPR)*, pages 13814–13823, June 2021.
- [38] B. Knott, S. Venkataraman, A. Hannun, S. Sengupta, M. Ibrahim, and L. van der Maaten. Crypten: Secure multi-party computation meets machine learning. *Advances in Neural Information Processing Systems*, 34:4961–4973, 2021.
- [39] A. Krizhevsky and G. Hinton. Learning multiple layers of features from tiny images. Technical Report 001, University of Toronto, 2009.
- [40] J.-W. Lee, H. Kang, Y. Lee, W. Choi, J. Eom, M. Deryabin, E. Lee, J. Lee, D. Yoo, Y.-S. Kim, et al. Privacy-preserving machine learning with fully homomorphic encryption for deep neural network. *IEEE Access*, 10:30039–30054, 2022.
- [41] Q. Li, Z. Shen, Z. Qin, Y. Xie, X. Zhang, T. Du, and J. Yin. Translinkguard: Safeguarding transformer models against model stealing in edge deployment, 2024.
- [42] Y. Li, H. Wang, and M. Barni. A survey of deep neural network watermarking techniques. *Neurocomputing*, 461:171–193, 2021.
- [43] N. Lin, X. Chen, H. Lu, and X. Li. Chaotic weights: A novel approach to protect intellectual property of deep neural networks. *IEEE Transactions on Computer-Aided Design of Integrated Circuits and Systems*, 2020.
- [44] J. Liu, M. Juuti, Y. Lu, and N. Asokan. Oblivious neural network predictions via minionn transformations. In *Proceedings of the 2017 ACM SIGSAC Conference on Computer and Communications Security, CCS '17*, page 619–631, New York, NY, USA, 2017. Association for Computing Machinery.

- [45] X. Ma, G. Fang, and X. Wang. Llm-pruner: On the structural pruning of large language models. In A. Oh, T. Naumann, A. Globerson, K. Saenko, M. Hardt, and S. Levine, editors, *Advances in Neural Information Processing Systems*, volume 36, pages 21702–21720. Curran Associates, Inc., 2023.
- [46] S. Meftah, B. H. M. Tan, C. F. Mun, K. M. M. Aung, B. Veeravalli, and V. Chandrasekhar. Doren: toward efficient deep convolutional neural networks with fully homomorphic encryption. *IEEE Transactions on Information Forensics and Security*, 16:3740–3752, 2021.
- [47] F. Meng, Z. Wang, and M. Zhang. Pissa: Principal singular values and singular vectors adaptation of large language models. *arXiv preprint arXiv:2404.02948*, 2024.
- [48] S. Merity, C. Xiong, J. Bradbury, and R. Socher. Pointer sentinel mixture models, 2016.
- [49] Microsoft Research. Phi-2: The surprising power of small language models. Language model with outstanding reasoning and language understanding capabilities, 2023.
- [50] A. Mok. ChatGPT could cost over \$700,000 per day to operate, 2023. [Accessed 22-05-2024].
- [51] S. Obla, X. Gong, A. Aloufi, P. Hu, and D. Takabi. Effective activation functions for homomorphic evaluation of deep neural networks. *IEEE access*, 8:153098–153112, 2020.
- [52] D. Oliynyk, R. Mayer, and A. Rauber. I know what you trained last summer: A survey on stealing machine learning models and defences. *ACM Comput. Surv.*, 55(14s), jul 2023.
- [53] G. Onoufriou, P. Mayfield, and G. Leontidis. Fully homomorphically encrypted deep learning as a service. *Machine Learning and Knowledge Extraction*, 3(4):819–834, 2021.
- [54] R. Perrault and J. Clark. Artificial intelligence index report 2024. 2024.
- [55] F. A. Petitcolas. Kerckhoffs’ principle. In *Encyclopedia of Cryptography, Security and Privacy*, pages 1–2. Springer, 2023.
- [56] B. Pulido-Gaytan, A. Tchernykh, J. M. Cortés-Mendoza, M. Babenko, G. Radchenko, A. Avetisyan, and A. Y. Drozdov. Privacy-preserving neural networks with homomorphic encryption: C hallenges and opportunities. *Peer-to-Peer Networking and Applications*, 14(3):1666–1691, 2021.
- [57] A. Pyone, M. Maung, and H. Kiya. Training dnn model with secret key for model protection. In *2020 IEEE 9th Global Conference on Consumer Electronics*, pages 818–821, 2020.
- [58] A. Radford, J. Wu, R. Child, D. Luan, D. Amodei, I. Sutskever, et al. Language models are unsupervised multitask learners. *OpenAI blog*, 1(8):9, 2019.
- [59] D. Rathee, M. Rathee, N. Kumar, N. Chandran, D. Gupta, A. Rastogi, and R. Sharma. Cryptflow2: Practical 2-party secure inference. In *Proceedings of the 2020 ACM SIGSAC Conference on Computer and Communications Security*, pages 325–342, 2020.
- [60] M. Ribeiro, K. Grolinger, and M. A. M. Capretz. MLaaS: Machine learning as a service. In *Proceedings of the 14th IEEE International Conference on Machine Learning and Applications*, pages 896–902, 2015.

- [61] B. D. Rouhani, M. S. Riazi, and F. Koushanfar. Deepsecure: scalable provably-secure deep learning. In *Proceedings of the 55th Annual Design Automation Conference, DAC '18*, New York, NY, USA, 2018. Association for Computing Machinery.
- [62] A. Sanyal, M. Kusner, A. Gascon, and V. Kanade. Tapas: Tricks to accelerate (encrypted) prediction as a service. In *International conference on machine learning*, pages 4490–4499. PMLR, 2018.
- [63] A. Schlögl and R. Böhme. ennclave: Offline inference with model confidentiality. In *Proceedings of the 13th ACM Workshop on Artificial Intelligence and Security*, pages 93–104, 2020.
- [64] A. Shamir, I. Canales-Martinez, A. Hambitzer, J. Chavez-Saab, F. Rodrigez-Henriquez, and N. Satpute. Polynomial time cryptanalytic extraction of neural network models, 2023.
- [65] P. Sharma, J. T. Ash, and D. Misra. The truth is in there: Improving reasoning in language models with layer-selective rank reduction, 2023.
- [66] J. Stallkamp, M. Schlipsing, J. Salmen, and C. Igel. The german traffic sign recognition benchmark: A multi-class classification competition. In *The 2011 International Joint Conference on Neural Networks*, pages 1453–1460. IEEE, 2011.
- [67] Z. Sun, R. Sun, L. Lu, and A. Mislove. Mind your weight (s): A large-scale study on insufficient machine learning model protection in mobile apps. In *30th USENIX security symposium (USENIX security 21)*, pages 1955–1972, 2021.
- [68] K. Szentannai, J. Al-Afandi, and A. Horváth. Preventing neural network weight stealing via network obfuscation. In *Intelligent Computing: Proceedings of the 2020 Computing Conference, Volume 3*, pages 1–11. Springer, 2020.
- [69] R. Taori, I. Gulrajani, T. Zhang, Y. Dubois, X. Li, C. Guestrin, P. Liang, and T. B. Hashimoto. Stanford alpaca: An instruction-following llama model, 2023.
- [70] H. Touvron, L. Martin, K. Stone, P. Albert, A. Almahairi, Y. Babaei, N. Bashlykov, S. Batra, P. Bhargava, S. Bhosale, et al. Llama 2: Open foundation and fine-tuned chat models. *arXiv preprint arXiv:2307.09288*, 2023.
- [71] J.-B. Truong, P. Maini, R. J. Walls, and N. Papernot. Data-free model extraction. In *Proceedings of the IEEE/CVF conference on computer vision and pattern recognition*, pages 4771–4780, 2021.
- [72] Y. Uchida, Y. Nagai, S. Sakazawa, and S. Satoh. Embedding watermarks into deep neural networks. In *Proceedings of the 2017 ACM on international conference on multimedia retrieval*, pages 269–277, 2017.
- [73] X. Wang, Y. Zheng, Z. Wan, and M. Zhang. Svd-llm: Truncation-aware singular value decomposition for large language model compression. *arXiv preprint arXiv:2403.07378*, 2024.
- [74] H. Xiao, K. Rasul, and R. Vollgraf. Fashion-MNIST: A novel image dataset for benchmarking machine learning algorithms. *arXiv:1708.07747*, 2017.
- [75] H. Xu, Y. Su, Z. Zhao, Y. Zhou, M. R. Lyu, and I. King. Deepobfuscation: Securing the structure of convolutional neural networks via knowledge distillation. *arXiv preprint arXiv:1806.10313*, 2018.

- [76] M. Xue, Z. Wu, Y. Zhang, J. Wang, and W. Liu. Advparams: An active dnn intellectual property protection technique via adversarial perturbation based parameter encryption. *IEEE Transactions on Emerging Topics in Computing*, 2022.
- [77] Y. Yan, X. Pan, M. Zhang, and M. Yang. Rethinking {White-Box} watermarks on deep learning models under neural structural obfuscation. In *32nd USENIX Security Symposium (USENIX Security 23)*, pages 2347–2364, 2023.
- [78] P. Yang, Y. Lao, and P. Li. Robust watermarking for deep neural networks via bi-level optimization. In *Proceedings of the IEEE/CVF International Conference on Computer Vision*, pages 14841–14850, 2021.
- [79] Y. Yao, J. Duan, K. Xu, Y. Cai, Z. Sun, and Y. Zhang. A survey on large language model (llm) security and privacy: The good, the bad, and the ugly. *High-Confidence Computing*, 4(2):100211, 2024.
- [80] D. Ye, P. Liu, and J. Xu. How fast can we obfuscate using ideal graded encoding schemes. Cryptology ePrint Archive, Paper 2017/321, 2017. <https://eprint.iacr.org/2017/321>, see also <https://www.esat.kuleuven.be/cosic/blog/program-obfuscation/>.
- [81] J. Zhang, Z. Gu, J. Jang, H. Wu, M. P. Stoecklin, H. Huang, and I. Molloy. Protecting intellectual property of deep neural networks with watermarking. In *Proceedings of the 2018 on Asia conference on computer and communications security*, pages 159–172, 2018.
- [82] L. Zhang, C. Li, Q. Hu, J. Lang, S. Huang, L. Hu, J. Leng, Q. Chen, and C. Lv. Enhancing privacy in large language model with homomorphic encryption and sparse attention. *Applied Sciences*, 13(24), 2023.
- [83] W. X. Zhao, K. Zhou, J. Li, T. Tang, X. Wang, Y. Hou, Y. Min, B. Zhang, J. Zhang, Z. Dong, Y. Du, C. Yang, Y. Chen, Z. Chen, J. Jiang, R. Ren, Y. Li, X. Tang, Z. Liu, P. Liu, J.-Y. Nie, and J.-R. Wen. A survey of large language models, 2023.
- [84] M. Zhou, X. Gao, J. Wu, J. C. Grundy, X. Chen, C. Chen, and L. Li. Model obfuscation for securing deployed neural networks. *openreview*, 2022.
- [85] T. Zhou, Y. Luo, S. Ren, and X. Xu. NNSplitter: An active defense solution for DNN model via automated weight obfuscation. In A. Krause, E. Brunskill, K. Cho, B. Engelhardt, S. Sabato, and J. Scarlett, editors, *Proceedings of the 40th International Conference on Machine Learning*, volume 202 of *Proceedings of Machine Learning Research*, pages 42614–42624. PMLR, 23–29 Jul 2023.
- [86] T. Zhou, S. Ren, and X. Xu. Obfunas: A neural architecture search-based dnn obfuscation approach. In *Proceedings of the 41st IEEE/ACM International Conference on Computer-Aided Design*, pages 1–9, 2022.
- [87] I. Zimerman, M. Baruch, N. Drucker, G. Ezov, O. Soceanu, and L. Wolf. Converting transformers to polynomial form for secure inference over homomorphic encryption. *arXiv preprint arXiv:2311.08610*, 2023.

A Proofs

Recall **Lemma 1. 1**

For $\|\mathbf{W}e_{i+1}\mathbf{a}_i\|_\infty < L$, the noise reduction equation 5 satisfies

$$\text{mod}(\mathbf{W}_{i+1}^{\mathcal{D}}\mathbf{a}_i t, L) = \text{mod}\left(\mathbf{a}_{i+1}^{\mathcal{D}(\text{noisy})}t - \tilde{\Delta}_{i,t}, L\right),$$

namely, $\mathbf{a}_{i+1}^{\mathcal{D}}t = \mathbf{W}_{i+1}^{\mathcal{D}}\mathbf{a}_i t$.

Proof.

$$\begin{aligned} \mathbf{a}_{i+1}^{\mathcal{D}}t &= \text{mod}\left(\mathbf{a}_{i+1}^{\mathcal{D}(\text{noisy})}t - \tilde{\Delta}_{i,t}, L\right) \\ &= \text{mod}\left(\mathbf{W}_{i+1}^{\mathcal{D}}\mathbf{a}_i^{\text{(noisy)}}t - \mathbf{W}_{i+1}^{\mathcal{D}}\Delta_{i,t}, L\right) \\ &= \text{mod}\left(\mathbf{W}_{i+1}^{\mathcal{D}}\text{mod}(\mathbf{a}_i t + \Delta_{i,t}, L) - \mathbf{W}_{i+1}^{\mathcal{D}}\Delta_{i,t}, L\right) \\ &\stackrel{(1)}{=} \text{mod}\left(\underbrace{\mathbf{W}_{i+1}^{\mathcal{D}}(\mathbf{a}_i t + \Delta_{i,t})}_{(1)} - \mathbf{W}_{i+1}^{\mathcal{D}}\Delta_{i,t}, L\right) \\ &= \text{mod}\left(\mathbf{W}_{i+1}^{\mathcal{D}}\mathbf{a}_i t, L\right) \\ &\stackrel{(2)}{=} \underbrace{\mathbf{W}_{i+1}^{\mathcal{D}}\mathbf{a}_i t}_{(2)} \end{aligned}$$

where, (1) follows from properties of modulo operator and (2) follows from the assumption that $\|\mathbf{W}e_{i+1}\mathbf{a}_i\|_\infty < L$. □

Now, we show that discrete uniform distribution $\mathbf{U}[0, L - 1]$ is closed to a constant addition modulo L .

Lemma 4 (Uniform Distribution Closeness). *Given a constant $s \in \mathbb{Z}^d$, random variable $n \sim \mathbf{U}[0, L - 1]^d$, and a random variable $x = \text{mod}(s + n, L)$, it holds $x \sim \mathbf{U}[0, L - 1]^d$.*

Proof. We first prove it for one-dimensional case $d = 1$. It is enough to show

$$P(x = a) = P(\text{mod}(s + n, L) = a) = 1/L.$$

We separate analysis to two distinct cases: (1) $\text{mod}(s, L) \leq a$, and (2) $\text{mod}(s, L) > a$:

1. For $\text{mod}(s, L) \leq a$, the equation $\text{mod}(s + n, L) = a$ holds iff $n = a - s$. In this case,

$$P(\text{mod}(s + n, L) = a) = P(n = a - s) = 1/L.$$

2. Similarly, for $\text{mod}(s, L) > a$, equation $\text{mod}(s + n, L) = a$ holds iff $n = L - (\text{mod}(s, L) - a)$. So also this case,

$$P(\text{mod}(s + n, L) = a) = P(n = L - (\text{mod}(s, L) - a)) = 1/L.$$

Finally, for any dimension $d > 1$, by repeating the same analysis for each dimension, we get

$$P(x = a) = \prod_{i=1}^d P(x_i = a_i) = 1/L^d,$$

where x_i and a_i are i -th coordinate of d -dimensional vectors x and a . □

Recall **Theorem 2**.

Given a constant $s \in \mathbb{Z}^d$, random variable $n \sim \mathbf{U}[0, L-1]^d$, and a random variable $x = \text{mod}(s+n, L)$, it holds $x \sim \mathbf{U}[0, L-1]^d$.

Proof. First, we prove that $s_n \sim \mathbf{U}[0, L-1]^d$, for $v_1 \in \mathbb{Z}_L^d$

$$\begin{aligned} P(s_n = v_1) &= \sum_{v_3 \in \mathbb{Z}^d} P(s_n = v_1 | s = v_3) P(s = v_3) \\ &= \sum_{v_3 \in \mathbb{Z}^d} \frac{1}{L^d} P(s = v_3) \\ &= \frac{1}{L^d} \sum_{v_3 \in \mathbb{Z}^d} P(s = v_3) \\ &= \frac{1}{L^d}. \end{aligned}$$

Next, we prove the independence by showing that $P(s_n = v_1, s = v_2) = P(s_n = v_1)P(s = v_2)$, where $v_1 \in \mathbb{Z}_L^d$ and $v_2 \in \mathbb{Z}^d$.

$$P(s_n = v_1, s = v_2) = P(s_n = v_1 | s = v_2) P(s = v_2) = \frac{1}{L^d} P(s = v_2) = P(s_n = v_1) P(s = v_2).$$

Note that we used $P(s_n | s) = 1/L^d$ from Lemma 4 in both equations. □

Recall **Lemma 3**.

Given $n_i \sim \mathbf{U}[0, L-1]^d$ and $\alpha_i \in \mathbb{Z}_L$ co-prime to L for $i = 1..l$, $n_s = \text{mod}(\sum_{i=1}^l \alpha_i n_i, L)$ is distributed $\mathbf{U}[0, L-1]^d$.

Proof. We start from the observation that multiplication of \mathbb{Z}_L^d by co-prime of L modulo L creates permutation of \mathbb{Z}_L^d . Permutation mapping on \mathbb{Z}_L^d preserves the probability of each element of \mathbb{Z}_L^d , so $\alpha_i n_i$ is also distributed $\mathbf{U}[0, L-1]^d$.

Next, use 2, by applying it with $n = \alpha_1 n_1$ and $s = \sum_{i=2}^l \alpha_i n_i$. □

B Practical Considerations

B.1 Pseudo-random numbers generation

In the main paper, we analyzed our protocol assuming true randomness from uniform distributions. However, in practice, we would use a Cryptographically Secure Pseudorandom Number Generator (CSPRNG). A CSPRNG has the property that no polynomial time adversary can distinguish between true uniform distribution and the output of such a generator except with a negligible probability. By using such a generator, our security proofs will continue to hold. Otherwise, an adversary that breaks security of our schemes can be used to construct a distinguisher that breaks the security of a CSPRNG.

B.2 Model partitioning

Model Partitioning MP receives a list of hyper-parameter triplets that define the how to perform a model partition:

$$[[\mathbf{block}, \mathbf{layer_type}, \mathbf{K}]_1, \dots, [\mathbf{block}, \mathbf{layer_type}, \mathbf{K}]_n]$$

where \mathbf{block} is any decoder block within an LLM, $\mathbf{layer_type}$ is any layer out of the possible layers in a decoder block, and \mathbf{K} is the number of top singular vectors to excise. Each triplet defines where singular vectors should be excised and how many. Therefore, using the list, MP partitions a given LLM into a secret version, comprised of the components detailed in the list, and an exposed version, comprised of all remaining components. Finding the optimal list with which to perform the partition is an optimization problem, that should consider trade-offs between the three following metrics: model security level, compute offload, and latency. For example, increasing security, given by excising a larger amount of singular vectors, comes at a cost of less compute offload. Additionally, choosing more layers on which to perform partition results in additional networking latency. In this paper, we evaluated several partitions, taking into account experimental findings in Section 4. For example, we realised it is useful to focus on first and latter blocks of the decoder backbone, and that it is enough to focus on a small amount of singular vectors. However, optimized partitions could be reached by incorporating Reinforcement Learning, Genetic Algorithms or additional heuristics.

C Compute & latency analysis details

In this analysis, we evaluate the inference latency of a neural network model that is partitioned between an edge device and the cloud according to the protocol suggested in the paper. This setup necessitates considering both computational latency and data transfer latency between the two compute resources. To accurately measure the total latency, we break down the protocol into distinct phases and calculate the computations in each, which contribute to the overall latency. Key parameters influencing latency include the bandwidth between the edge and cloud, the number of layers, the processor FLOPs capacity, and the size of the data being transferred. The formulas used for latency approximation are given by:

Computation Time (T_{Compute}): The time required to perform the necessary computations on the edge or cloud.

$$T_{\text{Compute}} = \frac{\text{FLOPs}}{\text{HardwareFLOP/s} \times \text{Utilization}} \quad (1)$$

Data Transfer Time (T_{Transfer}): The time required to transfer data between the edge and the cloud.

$$T_{\text{Transfer}} = \lambda_a + \frac{\text{input_size} \times b \times s}{\text{Bandwidth}} \quad (2)$$

Where λ_a is the network latency between the edge and the cloud, b is the batch size, and s is the size of each activation value in bytes.

Note that we chose to keep the SVD-decomposed weight matrix W_{c_i} decomposed in the cloud as $U_{c_i} \Sigma_{c_i} V_{c_i}$. This decision is based on the assumption that $k \ll m, n$, which makes the amount of computation lower than performing a full matrix multiplication. Conversely, we decided to reconstruct W_{e_i} after decomposition for use on the edge device because in this scenario, using the reconstructed matrix on the edge results in less computation compared to operating with the decomposed form.

C.1 Total latency calculation

Since the processing of each phase is sequential and cannot be parallelized, the total latency is the sum of the individual latency of each phase. This ensures that the computation and data transfer steps are accounted for in a linear sequence, reflecting the actual flow of operations during inference.

The total latency (T_{Total}) for the purposed protocol, where the model is partitioned between an edge device and a cloud server, can be divided into three main components: edge computations (P^e), cloud computation (P^c), and data transfer (P^t).

Edge Computation are given by

$$\text{FLOPS}^{\text{edge}} = (l - l_d) \cdot P_{\text{non-dec}}^e + l_d \cdot P_{\text{compute}}^e = 2mnb \cdot l + nb \cdot (l - l_d) \quad (3)$$

Where l_d represents the decomposed layers and l represents the total layers in the model. With regards to the full model on the edge, we find that

$$\text{FLOPS}^{\text{full}} = 2mnb \cdot l + nb \cdot l \quad (4)$$

So the cloud offload consists of $n \cdot l_d$ activation operations.

Cloud Computation are given by

$$\begin{aligned} \text{FLOPS}^{\text{cloud}} &= l_d \cdot \left(P_{\text{compute}}^c + P_{\text{composed}}^c + P_{\text{noise_gen}}^c + P_{\text{noise_add}}^c \right) \\ &= 2l_d \cdot b \cdot (mk + nk + 2nl_v + 1.5n) \end{aligned} \quad (5)$$

Data Transfer is given by

$$N^{\text{transfer}} = P_{\text{input}}^t + l_d \cdot (P_{\text{upload}}^t + P_{\text{download}}^t) = nb(2l_d + 1) \quad (6)$$

Total Latency is given by

$$T_{\text{Total}} = T_{\text{Compute}}(\text{FLOPS}^{\text{edge}}) + T_{\text{Compute}}(\text{FLOPS}^{\text{cloud}}) + T_{\text{Transfer}}(N^{\text{transfer}}) \quad (7)$$

C.2 Selecting parameter values

Next, we will select specific values for the parameters used in the formulas and analyze the results. This will help illustrate the computational and data transfer latency in our protocol, when the weights are split between an edge device and a cloud server. We based many of our numbers on Llama2 model, treating it as if it were a regular feedforward (FF) network to simplify the analysis and make the estimations more straightforward. Additionally, we assumed a single token generation and chose the one of the decomposition strategies mentioned in the Experiments section as an efficient and robust option.

C.3 Results

The results of our calculations are as follows, and are discussed in the paper itself in section 5.

D Probabilistic analysis precomputed vector repeating

To analyze the chance to get the same selection of $\mathbf{z}_{j,i}$, we first compute $C(N, \ell)$ the total number of possible combination to selecting ℓ vectors out of N ,

$$C(N, \ell) = \frac{N!}{(N - \ell)! \ell!}.$$

The chance to get the same combination of $\mathbf{z}_{j,i}$ equals

$$\begin{aligned} & P(\exists t_1, t_2 \text{ such that } t_1 < t_2 < n, \text{ so } S_{i,t_1} = S_{i,t_2}) \\ &= 1 - P(\nexists t_1, t_2 \text{ such that } t_1 < t_2 < n, \text{ so } S_{i,t_1} = S_{i,t_2}) \\ &= 1 - \frac{C(N, \ell)!}{C(N, \ell)^n (C(N, \ell) - n)!} \end{aligned}$$

For $N = 10^6$, $\ell = 50$ and $n = 10^{15}$, $C(10^6, 50) = 3.28E235$. Applying the above equation directly is not practical because for a very large $C(10^6, 50)$ value, so instead we can use the following approximation

$$\begin{aligned} 1 - \frac{C(N, \ell)!}{C(N, \ell)^n (C(N, \ell) - n)!} &< 1 - \left(\frac{C(N, \ell) - n}{C(N, \ell)}\right)^n \\ &= 1 - \left(1 - \frac{n}{C(N, \ell)}\right)^n \\ &\sim 1 - \left(1 - \frac{n^2}{C(N, \ell)}\right) \\ &= \frac{n^2}{C(N, \ell)} \\ &\sim 10^{-206} \end{aligned}$$

E Illustration of secret masking

E.0.1 Minimal number of Singular Vectors that must be decomposed

The following lemma shows that under the use of SVD decomposition, more than one singular vector is needed to be removed from the model and stored separately on the cloud, noted by W_c .

Lemma 5 (The minimal number of required singular vectors to be hidden). *The matrix V_c should contain more than one singular vector, in order to ensure that an attacker cannot reconstruct W_c using only the singular vector available to them on the edge in W_e , or that they are combinatorially complex for the user to reconstruct.*

Proof. Let us denote

$$W_e = S_e V_e D_e = \begin{pmatrix} \text{---} & S_1 & \text{---} \\ \text{---} & S_2 & \text{---} \\ \text{---} & S_3 & \text{---} \\ & \vdots & \\ \text{---} & S_n & \text{---} \end{pmatrix} \cdot \begin{pmatrix} \sigma_1 & 0 & 0 & \cdots & 0 \\ 0 & \sigma_2 & 0 & \cdots & 0 \\ 0 & 0 & \sigma_3 & \cdots & 0 \\ \vdots & \vdots & \vdots & & \vdots \\ 0 & 0 & 0 & \cdots & \sigma_n \end{pmatrix} \cdot \begin{pmatrix} \text{---} & D_1 & \text{---} \\ \text{---} & D_2 & \text{---} \\ \text{---} & D_3 & \text{---} \\ & \vdots & \\ \text{---} & D_n & \text{---} \end{pmatrix}^t$$

Let us suppose that one singular vector (without the loss of generally the largest one), namely S_1 , should be enough to be designated for the matrix W_c , ensuring W_c is unrecoverable to an attacker.. Then, in the edge device, we have $n - 1$ orthonormal vectors in $\{S_2, S_3, \dots, S_n\}$. Since all vectors in it are orthonormal it could be leveraged to construct the following $n - 1$ equations,

$$\begin{aligned} S_2^t \cdot S_1 &= 0 \\ S_3^t \cdot S_1 &= 0 \\ &\vdots \\ S_n^t \cdot S_1 &= 0, \end{aligned}$$

which results in only one degree of freedom. Now, simply applying the Gram-Schmidt process (or any other orthonormalization techniques) would result in the exact S_1 singular vector. This is in contradiction to the assumption. \square

Remark 2 (Finding the corresponding missing singular vector). *The sum of the singular values of a matrix equals the trace of that matrix, meaning $\text{trace}(W_e) = \lambda_1 + \lambda_2 + \dots + \lambda_{n-1} + \lambda_n$. Given $\lambda_2, \lambda_3, \dots, \lambda_{n-1}$, the first singular value could be computed by*

$$\lambda_1 = \text{trace}(W_e) - (\lambda_2 + \lambda_3 + \dots + \lambda_n)$$

Corollary 5.1. *Directly by lemma 5, separating $n \gg k \geq 2$ singular values and their corresponding singular vectors into their cloud designated matrices S_c, V_c, D_c , results in k equations with n unknown parameters. Thus, in this case, the level of freedom that can not be retrieved (by linear algebraic operations) can given by $n - k + 1$.*

F Equivalence of Convolutional Layer and Fully Connected Layer

Convolutional Layer

Consider the input tensor \mathbf{X} of shape (H, W, C) , the convolutional kernel \mathbf{K} of shape (kH, kW, C, N) , and the output tensor \mathbf{O} of shape (H_o, W_o, N) . For simplicity, assume stride $s = 1$ and no padding.

The output at position (i, j) for filter n is given by:

$$\mathbf{O}_{i,j,n} = \sum_{c=1}^C \sum_{u=1}^{kH} \sum_{v=1}^{kW} \mathbf{X}_{i+u-1, j+v-1, c} \cdot \mathbf{K}_{u,v,c,n}$$

Fully Connected Layer

The equivalent fully connected layer will have an input vector \mathbf{x} and a weight matrix \mathbf{W} . The input tensor \mathbf{X} is unrolled into a vector \mathbf{x} of size $H \cdot W \cdot C$.

Unrolling Process

1. Flatten the Input:

$$\mathbf{x} = \text{vec}(\mathbf{X})$$

2. **Construct the Weight Matrix:** The weight matrix \mathbf{W} for the fully connected layer will be of shape $(H_o \cdot W_o \cdot N, H \cdot W \cdot C)$. Each row of \mathbf{W} corresponds to a specific position of the kernel applied to the flattened input.

For each output position (i, j) and filter n :

$$\mathbf{W}_{n, \text{index}(i, j, c)} = \mathbf{K}_{u, v, c, n}$$

where $\text{index}(i, j, c)$ maps the 3D position (i, j, c) in the input tensor to the corresponding position in the flattened vector.

Analytical Formulation

For each output position (i, j) and filter n :

$$\mathbf{O}_{i, j, n} = \sum_{c=1}^C \sum_{u=1}^{kH} \sum_{v=1}^{kW} \mathbf{X}_{i+u-1, j+v-1, c} \cdot \mathbf{K}_{u, v, c, n}$$

Unroll \mathbf{X} to \mathbf{x} and define the corresponding weight vector $\mathbf{w}_{(i, j, n)}$ in \mathbf{W} :

$$\mathbf{w}_{(i, j, n)} = \text{vec}(\mathbf{K}_{:, :, c, n})$$

The output \mathbf{O} is obtained by matrix multiplication:

$$\mathbf{o} = \mathbf{W} \cdot \mathbf{x}$$

where \mathbf{o} is the flattened version of \mathbf{O} .

Table 1: Description of phases and operations

Phase	Op Type	Frequency	Description	FLOPs/Data Size
Upload Input	Transfer	Once	Transfer input data X of size n to the cloud	$n \times b$
Edge-Only Compute	Compute	Each non-decomposed layer	Compute all non-decomposed operations for matrices W_{e_i}	$2 \cdot m \cdot n \cdot b + n \cdot b$
Edge-Partial Compute	Compute	Each decomposed layer	Weights Matrix Multiplication $W_{e_{i+1}} a_{i_{\text{noisy}}}$	$2 \cdot m \cdot n \cdot b$
Cloud-Partial Compute	Compute	Each decomposed layer	Decomposed Matrices Multiplication $U_c \Sigma_c V_c a_i$	$2 \cdot k \cdot b \cdot (m + n)$
Upload Edge to Cloud	Transfer	Each decomposed layer	Transfer edge activation $a_{e,i+1_{\text{noisy}}}$ data to the cloud	$n \times b$
Cloud Activation Function	Compute	Each decomposed layer	Remove Noise + Vector addition + activation $a_{i+1} = \sigma(a_{c_i} + a_{e_i} - \tilde{\Delta}_i)$	$2 \cdot n \cdot b \cdot (L_v + 1)$
Cloud Noise Vector Generation	Compute	Each decomposed layer	Sample L_v noise vectors and create Δ_i	$2 \cdot n \cdot b \cdot L_v$
Cloud Noise Addition	Compute	Each decomposed layer	Vector addition $a_{i_{\text{noisy}}} = a_i + \Delta_i$	$n \cdot b$
Activation Data Download	Transfer	Each decomposed layer	Transfer final activation data to edge $a_{i_{\text{noisy}}}$	$n \times b$

Table 2: Summary of model parameters, hardware specifications, and network details

Parameter	Value	Description
Model Parameters		
l : Total Layers	224	7 layers (4 attn + 3 mpl) per block Llama2 contains 32 blocks
l_d : Decomposed Layers	70	7 layers (4 attn + 3 mpl) per block 10 decomposed blocks in configuration X4
n, m : Matrix Dimensions	4096, 4096	Attention Layer
b : batch_size	32	Average input length
k : Secret Singular Values	50	X4 configuration
l_v : Sampled Noise Vectors	50	
s : Activation size in bytes	$4b$	FP32
Hardware Specifications		
Edge GPU FLOP/sec	4 TFlops/sec	Nvidia Jetson Nano spec (estimation for FP32)
Cloud GPU FLOP/sec	14 TFlops/sec	Nvidia V100 spec
Utilization	40%	Realistic estimation
Network Details		
B : Network Bandwidth	25 MB/s	Average bandwidth in the US
λ_a : Network Delay	35 ms	Average latency in the US Global IP Network Latency (att.net)

Table 3: Performance

Metric	Value
FLOPs Full Model	240.547 GFLOPs
FLOPs Edge (Hybrid)	240.538 GFLOPs
FLOPs Cloud (Hybrid)	3.697 GFLOPs
Input Transfer	1.848 M
Compute Edge Latency	150.34 ms
Compute Cloud Latency	0.66 ms
Transfer Latency	71.31 ms
Total Latency	222.31 ms